

An Off-the-shelf Electric Propulsion System for CubeSats

Craig Clark
Clyde Space Ltd
West of Scotland Science Park ,G20 OSP, Glasgow, UK
craig.clark@clyde-space.com

Francesco Guarducci, Michele Coletti
Mars Space Ltd
23 Spindlewood Close, SO16 3QD, Southampton, UK
francesco.guarducci@mars-space.co.uk
michele.coletti@mars-space.co.uk

Stephen B. Gabriel
University of Southampton
Astronautics Research Group, SO17 1BJ, Southampton, UK
sbg2@soton.ac.uk

ABSTRACT

Cubesats, allow cheap access to space and are one of the fastest growing sectors in the space industry. A pulsed plasma thruster to perform drag compensation for a Cubesat platform, with the aim of doubling the time needed for the Cubesat to naturally de-orbit (hence doubling its lifetime) is currently under development by Clyde Space Ltd, Mars Space Ltd and the University of Southampton under an ESA funded project. In this paper, mission requirements, the design of the thruster and the experimental results obtained up to now will be presented.

INTRODUCTION

Cubesats are one of the fastest growing sectors in the space industry, allowing for cheap access to space. They are normally launched into sun-synchronous or LEO orbits with an altitude of about 600-650 km. They are currently limited by their lack of orbit control and their lifetime is therefore determined by the natural, drag-induced, de-orbiting. Clyde Space Ltd, Mars Space Ltd and the University of Southampton have performed a study funded by the ESA ITI program to adapt a Teflon-fed Pulsed Plasma Thruster (PPT) to a 3U Cubesat with the aim of doubling its lifetime and consequently increasing its economical attractiveness. Ablative Pulsed Plasma Thrusters have been chosen as propulsion subsystem due to their high scalability in terms of geometry, power input, performance and also to their high reliability and ease of control. Developed in the late 60s, the PPTs represent the first example of electric propulsion successfully employed in space, with the Zond-2 (USSR) and the LES-6 (USA) the first satellites to use Plasma Thrusters [1]. From then on PPT development has continued focusing on both high energy and low energy devices [1-9].

In this paper the requirements, that such a propulsive subsystem must meet, will be derived, the design of the

thruster briefly presented and the experimental results obtained up to the present, are reported.

MISSION REQUIREMENTS

In this section the requirements that must be met by the PPT in terms of mass, dimensions, power and performance will be presented. The thruster and its electronics will be mounted on a PC104 standard PCB card that is normally adopted by the Cubesat Kit bus; hence the maximum dimensions allowable for the propulsive subsystem are 90×90×27 mm. Since the PCB cards are normally stacked horizontally one on top of the other the thrust direction will be along the 27 mm direction. Considering that a PC104 card has a thickness of 1.6 mm the maximum allowable length of the discharge chamber of the PPT will be 25mm.

Given the Cubesat tight mass budget (1kg for a 1U satellite and 3kg for a 3U satellite [10]), the mass of the whole thruster assembly including electronics, capacitors and propellant will be limited to 150 g margins included. Due to the limited mass available, the propellant (Teflon[®]) mass will be limited to 10 g. The power available is constrained by the limited solar panel extension on board of a Cubesat: a maximum limit has been fixed at 0.3 W of average power consumption.

The thruster will be required to compensate the drag induced de-orbiting for a period of at least 3 years at a nominal altitude of 600 km. Assuming a drag coefficient of 2.2 on a 3U cubesat the total impulse needed to fully compensate for three years of drag will be 28.4 Ns. Considering this value, Figure 1 shows the average specific impulse required to meet the mission requirements as a function of the available propellant mass.

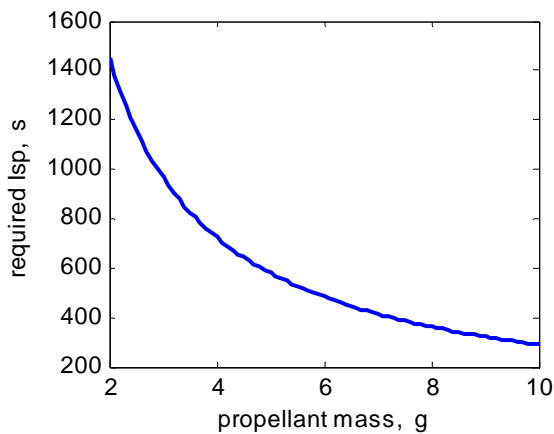


Figure 1: Required specific impulse as a function of propellant mass

Table 1: PPT requirements

Requirement	Value	Requirement	Value
Maximum volume	90×90×25 mm	Total impulse	28.4 Ns
Maximum mass	150 g	Average power	0.3 W
Maximum thruster length	25 mm	Mission duration	3 y
Maximum propellant mass	10 g	Minimum Isp	289.5 s

THRUSTER DESIGN

In this section the thruster design will be presented. Efforts were aimed at maximizing the thruster specific impulse, in order to reduce the required propellant mass and to provide margins on top of the requirements. Firstly the design of the PPT discharge chamber will be presented and then the design of the spark plug and of the thruster electronics will be reported.

Discharge Chamber Design

The first design choice is how to feed the propellant and hence if a side-fed or a breech-fed configuration is to be

used. According to the requirements the thruster discharge chamber maximum length is 25 mm. Since the total available length is already small, and considering that the choice of a breech-fed configuration would further reduce the available length to allow for propellant storage, the baseline design will be based on a side-fed configuration.

In many studies regarding the PPT functioning [1, 11], the electromagnetic acceleration component and efficiency are found to be respectively proportional to the inductance variation per unit length L' and to the ratio between the inductance variation during the discharge and the initial discharge circuit inductance $\Delta L/L_0$.

$$I_{bit_{em}} = \frac{1}{2} L' \Psi \quad \eta_{el} \leq \frac{\Delta L}{L_0} = \frac{L' d_{el}}{L_0} \quad (1)$$

Hence to maximize the thruster performance, L_0 must be minimized and L' maximized. The value of L_0 has been already minimized by choosing a side fed configuration that will allow the capacitors to be mounted right on the back of the discharge chamber; the value of L' will be maximized in the design of the electrodes.

In recent PPT research carried out in Europe [12, 13] tongue shaped electrodes has been successfully found to improve the value of L' and to maximize the electromagnetic part of the impulse bit. Nevertheless in this study we have decided to use a more “conservative” approach and to use rectangular electrodes given the wider use that this kind of electrodes have had in the past [1, 14-19]. The value of the inductance variation per unit length, L' for rectangular electrodes can be calculated in $\mu\text{H}/\text{m}$ as [20]

$$L' = 0.6 + 0.4 \ln \frac{h}{w+t} \quad (2)$$

or according to another approach using a conformal mapping technique [21] the value of L' can be plotted for various h/w ratios as reported in Figure 2.

According to both approaches to maximize L' the electrode spacing must be increased and the electrode width and thickness decreased. However, if the value of h/w is too high, important non uniformities may arise in the electro-magnetic field, thus reducing the acceleration process efficiency [22]. Considering what has been said above and the values that can be found in the literature [1], an h/w ratio equal to 2 has been chosen for the design of the PPT electrodes. The electrodes will not be parallel for their whole length but

will diverge from half way of their length to create a nozzle to maximize the thermodynamic component of thrust.

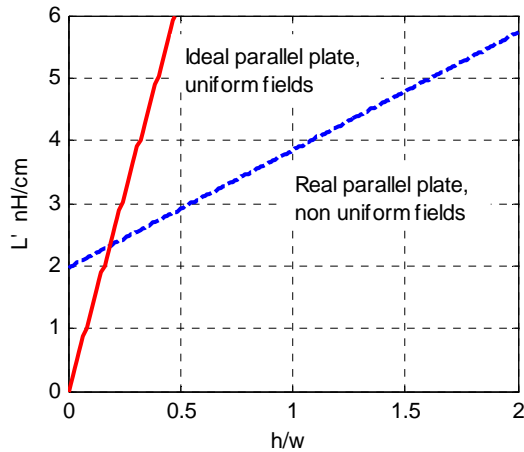


Figure 2: Inductance per unit length trend with h/w ratio [23]

For the electrode material a copper-tungsten (70% W – 30% Cu) alloy has been selected. This material has been chosen for its low electrical resistivity (37 nΩm), good mechanical and thermal properties and reduced erosion rates [11, 23].

To complete the geometrical design of the thruster, the propellant bar dimensions and the shot energy must be selected. In many of the past studies involving both side-fed and breech-fed PPTs [1, 24-27], one of the main parameters found to affect the thruster performances in terms of propellant consumption and specific impulse is the ratio of the discharge energy to the propellant area exposed to the discharge E/A ; the higher the energy per area ratio the higher the values of the specific impulse. In particular many authors [1, 24-27] found that the specific impulse varies less than linearly with E/A . Semi-empirical relations have been derived by Guman [1, 25, 26] (using data relative to different configurations of the same thruster) and by Gessini and Paccani [26] (using data relative to many different thrusters).

Considering that the curve obtained from the scaling laws reported in [25] predicts lower values of the I_{sp} , to perform a conservative design from now on only this scaling law will be used.

If we now consider that, given the limited available volume, the maximum length of each propellant bar is about 3.5 cm and that an excessive value of the E/A ratio will translate into a reduced propellant area and hence in long propellant bars (to keep the amount of propellant constant at 10g) the data reported in Figure 1

and 3 can be combined to derive the trend of the I_{sp} required to accomplish the mission with E/A for different shot energies (Figure 4).

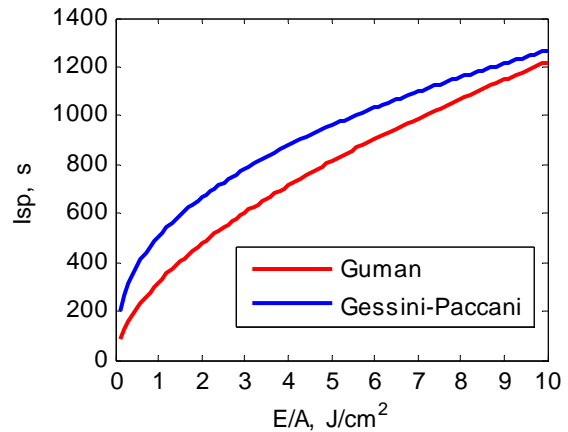


Figure 3: Semi-empirical specific impulse trend with E/A

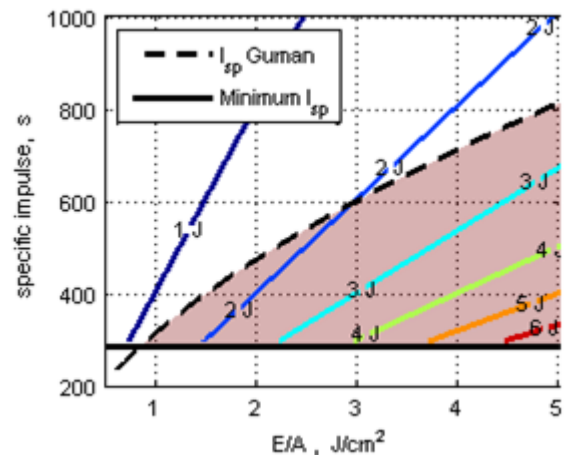


Figure 4: Required specific impulse trend with E/A for different values of the shot energy E

It must be noted that, for every energy level, the required specific impulse curve collapses on the 289.5 s value below a certain value of the E/A ratio. This is because as E/A decreases the propellant surface (and hence the propellant mass) increases. This is acceptable only up to 10 g (as specified in the requirements and that is equivalent to an I_{sp} of 289.5 s), any further decrease of the E/A ratio will result in a decrease in the propellant bar length (to preserve the 10 g maximum propellant limit). Such combinations of E/A and E have been judged to be non desirable since not all the volume allocated for the thruster will be used.

The specific impulse predicted by the Guman semi-empirical scaling law has been also shown in Figure 4.

To meet the performance requirements, the specific impulse expected by the PPT (i.e. the one predicted by Guman) must be higher than the one required to accomplish the mission (correspondent to the shot energy and propellant area chosen); hence the choice of the E/A and E values should be done to obtain a required specific impulse in the highlighted area in Figure 4. As a result only energy values larger than 1.5 J are allowed.

Considering what is given in Figure 4 and that the shot energy will drive the capacitor mass and volume, a discharge energy slightly over 2 J and a E/A ratio of the order of 2 have been chosen with a propellant mass (given by the maximum allowable bar length) of about 7.7g. This combination of E/A and shot energy values should produce an Isp of about 500s in comparison to a required Isp of about 410s, hence providing a safety margin of about 20%. In addition to this, the chosen E/A ratio is in agreement with the values used in other low energy PPTs[1].

Spark Plug Design

A spark plug is needed to initiate the PPT discharge. The main difficulty in the design of the spark plugs for this thruster is the small dimensions of the electrodes. Spark plugs have normally a concentric design [28] with a central electrode connected to a high voltage supply (usually up to about 10kV) surrounded by a layer of semiconductor material (or Teflon[®]) and are inserted in one of the thruster electrodes as shown in Figure 5.

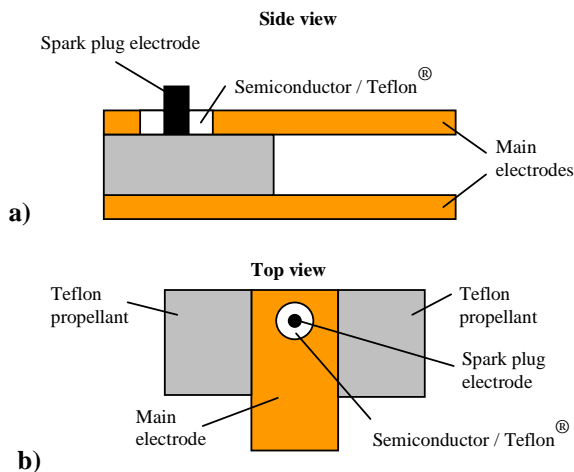


Figure 5: Diagram of a “conventional” spark plug setup: (a) side view, (b) top view

In such a setup the discharge may happen at any point along the electrode/semiconductor circumference. This is tolerable and will cause small shot to shot variation given that the propellant length is much bigger than the

spark plug size. In the case of our PPT, given the small dimension of the electrodes and of the propellant bars, the spark plug should be extremely small and therefore difficult to manufacture. To overcome this problem a rectangular spark plug has been designed. A sketch representing a top view of such design is shown below.

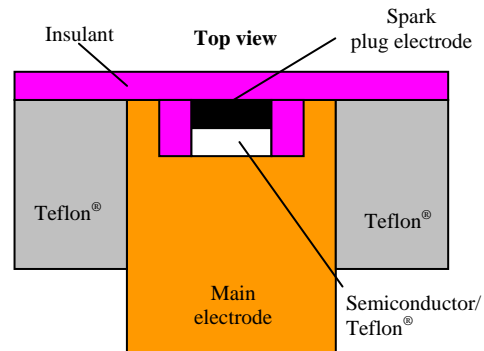


Figure 6: Spark plug diagram

With this design the discharge will occur somewhere along the spark plug electrode width but will be localized at the beginning of the main propellant bar (about 0.5 mm from its edge) hence assuring that the main discharge will sweep along the whole propellant face. The spark plug will be operated with a discharge energy of 0.01 J with voltages up to 15 kV. Similar values for spark plug Teflon propellant dimensions and spark plug voltages were employed on Unisat5 PPT[29] and proved to work properly.

Electronics Design

The PPT is powered and controlled by an electronics board designed and manufactured by Clyde Space Ltd. An LT3750 flyback converter, specifically designed to charge large capacitors, is used to drive the main capacitor bank charging circuit, while a Cockcroft-Walton voltage multiplier is employed to feed the spark plug. The spark plug charging voltage can be regulated up to a maximum value of 15 kV. The main capacitor bank voltage instead can be controlled through a simple rheostat assuming values between 900 V and 1600 V.

Since the main capacitor bank and the spark plug charging circuits include fly-back transformers, the electronics board can be electrically isolated from the thruster electrodes. Hence, the thruster can be kept floating, thus avoiding noise and ground shifts that could be generated when the thruster is firing, damaging the electronics board.

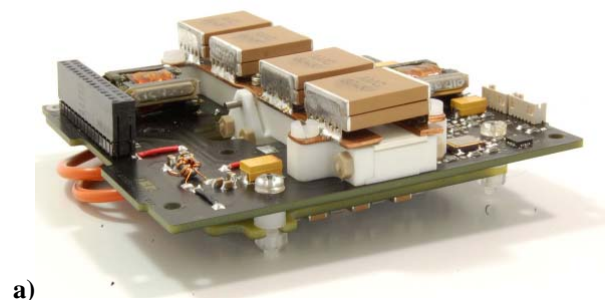
A PIC16 μ -controller commands and synchronizes the two charging circuits. The firing signal can be sent through a dedicated pin. Alternatively, a digital firing

command can be forwarded to the μ -controller via an I2C communication bus, which also allows monitoring and different charging parameters.

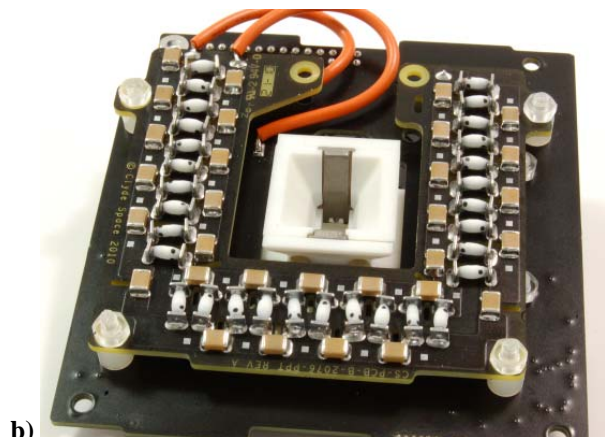
EXPERIMENTAL RESULTS

The PPT and the associated electronics have been built, assembled and tested. The tests have been carried out in a vacuum chamber about 0.35 m³ in volume. The pressure was maintained by the pumping system in a range between $3 \cdot 10^{-5}$ and $6 \cdot 10^{-5}$ mbar throughout the tests. The thruster was fed by the dedicated electronics board, which was specifically designed by Clyde Space to charge the PPT main capacitors and to power up the spark plug, providing synchronization between these processes and meeting the strict mass and volume budgets of a cubesat subsystem.

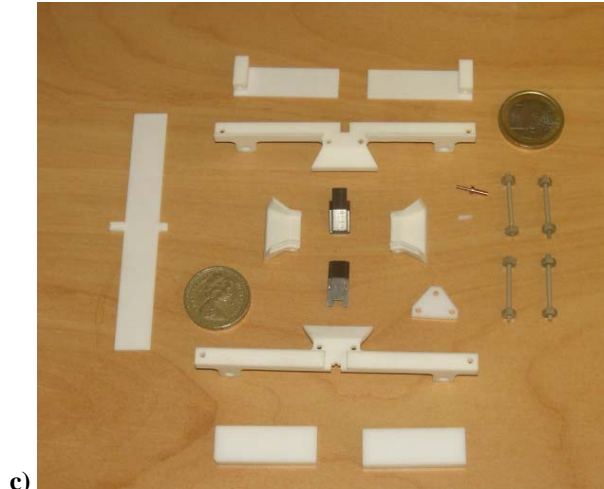
The voltage discharge curves were measured using two Tektronix high voltage probes and the discharge current curve using Rogowsky coils.



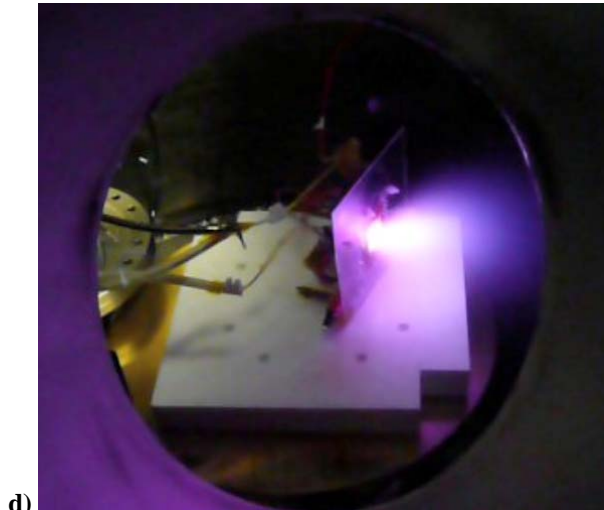
a)



b)



c)



d)

Figure 7: PPT. a) and b) assembled, c) disassembled discharge chamber, d) firing in the University of Southampton vacuum facility

Capacitor banks

Two capacitor banks have been assembled and tested. The first bank (“flight bank”) has been built using four 0.8 μ F high frequency pulse SMT capacitors rated up to 2000 V hence providing a total nominal bank capacitance of 3.2 μ F. The second bank (“test bank”) has been built using COTS components, selected because they have mass and volume similar to the more efficient (and expensive) flight capacitors. Each capacitor has a capacitance of 1 μ F and is rated up to 1000V hence a bank of 2.5 μ F rated up to 2000 V has been built using a parallel of five two-capacitors series. The two banks have been tested to measure their internal resistance R_0 and inductance L_0 and to verify the capacitance de-rating with voltage. The values of R_0 and L_0 have been measured at 0.1, 1 and 10 kHz and are reported in Figure 8, 9.

As it can be seen the trend is linear on a double logarithmic scale hence the value of L_0 and R_0 at the PPT discharge frequency can be calculated. Using the frequency value extrapolated from the discharge current and voltage curves (about 0.6 MHz) the value of initial inductance and resistance for the two banks are 22 nH and 3 m Ω for the test bank and 3 nH and 2 m Ω for the flight bank.

The lower L_0 value of the flight bank is justified not only by the higher standard of the capacitors but also by the fact that the test bank has been built such that Rogowsky coils can be fit in between the capacitors and the thruster power bus bars hence increasing the area of the discharge circuit and consequently increasing L_0 .

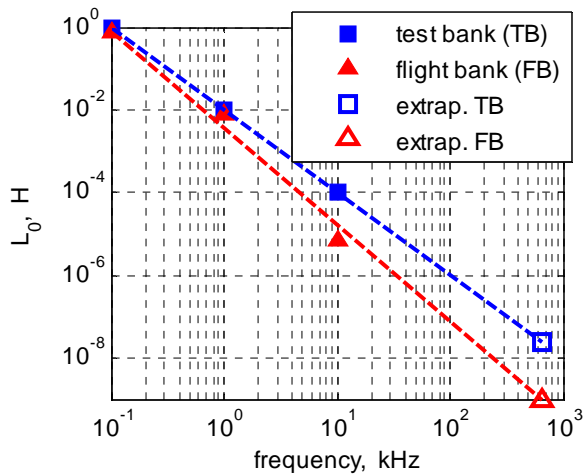


Figure 8: Capacitor bank initial inductance L_0 , the empty markers are extrapolated values

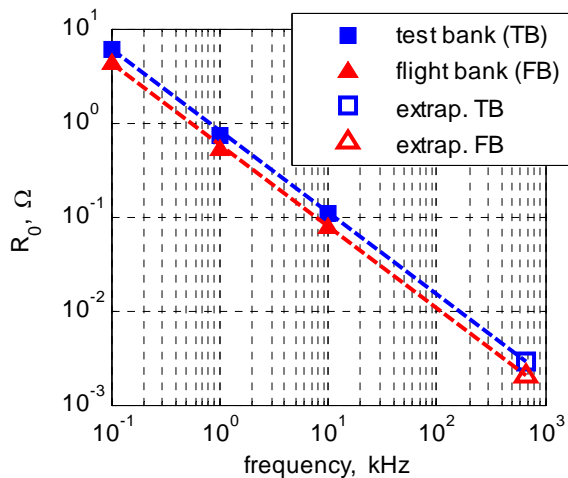


Figure 9: Capacitor bank initial resistance R_0 , the empty markers are extrapolated values

The capacitance trend with voltage of the two banks has also been investigated finding a de-rating at 2000V of about 40% for the flight bank and 70% for the test bank.

Spark Plug

The spark plug has been tested applying voltages from 1kV up to the maximum level allowed by the electronics of 15kV. The spark plug has proved reliable discharge initiation starting from a voltage of 3kV that increased with use up to 4-5kV still well below the maximum voltage capabilities of the electronics.

Discharge Current and Voltage Waveforms

The thruster has been fired at various energy levels with both the test and flight banks to measure the current and voltage waveforms. Unfortunately the flight capacitor bank failed after a few shots and hence no meaningful data could be gathered. This failure has been attributed to the excessive structural stresses relative to the mechanical response of the capacitor dielectric material (that showed piezoelectric properties) to the rapidly changing current. Consequently the tests have been carried out using only the test capacitor bank using six different values of the charge voltage between 950 V and 1550 V correspondent to energies between 1 and 2 J.

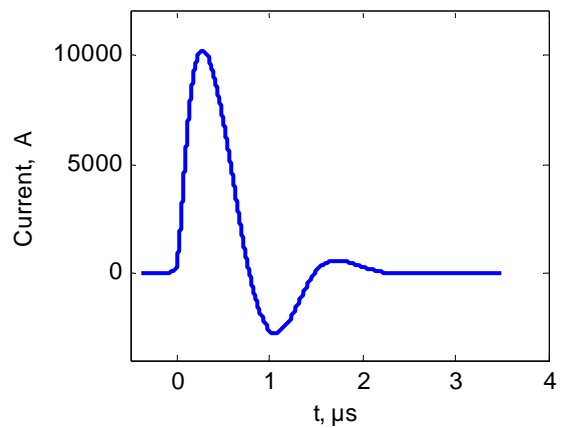


Figure 10: Discharge current curve ($E = 2 \text{ J}$)

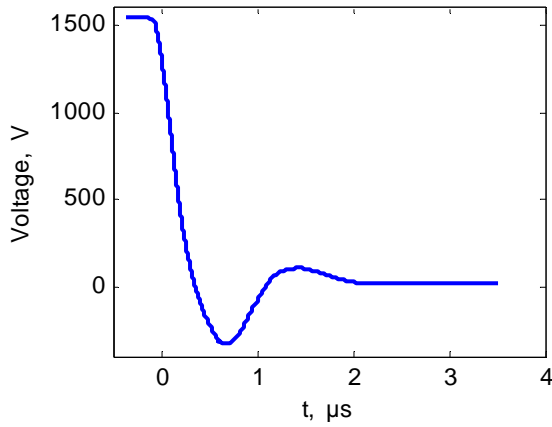


Figure 11: Discharge voltage curve (E = 2 J)

Figure 10 and 11 show the current and voltage curves, obtained averaging the data of ten different shots, for the 2 J energy. The discharge has an oscillatory behavior, showing, as in most of the PPTs [1], an impedance mismatch between the capacitors/feed lines and the plasma sheet that accelerates the propellant [1, 22]. This mismatch is determined by the constraints on the thruster initial inductance and on capacitance and initial voltage and directly affects the efficiency for electrical energy transfer [1, 22]. Moreover, the reversing current reduces the capacitor lifetime and the effectiveness of the ablation and acceleration processes [1, 15, 22]. However, it can be noticed that the current curve is completely damped after the first oscillation cycle, meaning that the system is not too far away from the optimal critical damping condition ($CR^2/4L = 1$) hence significantly reducing the negative effects described above. The voltage and the current measurement were also noticed to be very repeatable with a standard deviation of the first positive peak of the current curve of about 1.5 %, and a standard deviation of the first negative peak of about 6 %. The current and voltage curves have been interpolated representing the PPT as a fixed parameter RLC circuit [22] and hence fitting the experimental measurements to the functions

$$I = \frac{V_0}{\omega L} \sin(\omega t) \exp\left(-\frac{R}{2L} t\right) \quad (3)$$

$$V = \frac{V_0}{\omega C \sqrt{LC}} \sin(\omega t + \delta) \exp\left(-\frac{R}{2L} t\right) \quad (4)$$

Where ω and δ are

$$\omega = \sqrt{\frac{1}{LC} - \frac{R^2}{4L^2}} \quad \delta = \tan^{-1}\left(\frac{4L}{R^2 C} - 1\right)^{1/2} \quad (5)$$

The best fit values of R and L do not experience significant variations with the shot energy and are respectively 0.07 Ω and 20 nH producing an R-squared value for the fit of 0.993. As it can be noted the value of the resistance R is more than an order of magnitude bigger than the one relative to the capacitor bank and hence can be attributed almost entirely to the plasma resistance; the inductance value instead is in agreement with the value measured for the test capacitor bank.

The current parameter Ψ has also been evaluated for each of the tested energies. Its trend with the shot energy is reported in Figure 12.

As expected by previous studies [1, 26] the current parameter shows a linear trend with the discharge energy. The data has also been fitted using the formula proposed by Paulmbo and Guman [30]

$$\Psi = 1.3 \sqrt{\frac{C}{L_0}} E \quad (6)$$

where to obtain a best fit the multiplying coefficient has been increased from 1.3 to 1.45.

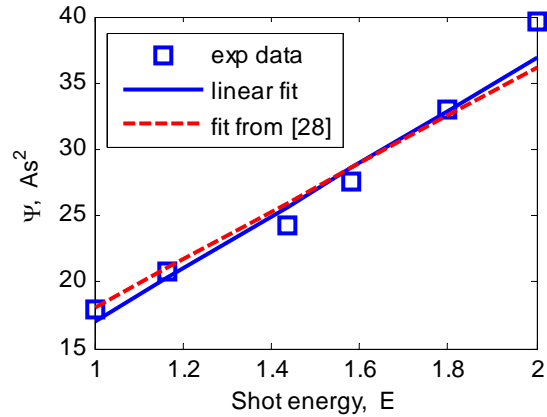


Figure 12: Current parameter trend with discharge energy

Impulse bit

The impulse bit of the thruster has also been measured. These measurements have been carried out at Institute of Space Systems, University of Stuttgart, Germany. The thrust balance used is an impulsive thrust balance [31-33] with a resolution that depends on the mass of the thrusters to be used and that in our case was about 1 μ Ns. The impulse bit has been measured for the energies of 1.6, 1.8 and 2J.

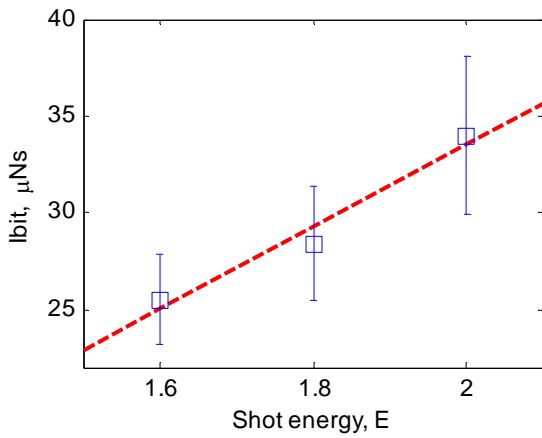


Figure 13: Ibit trend with shot energy

As it can be seen the Ibit shows a linear trend with energy as already pointed out in several experimental studies [1]. In particular a specific impulse bit of about $17 \mu\text{Ns}/\text{J}$ can be obtained from the data in Figure 13. The importance of the electromagnetic contribution to the impulse bit can be evaluated using the values of Ψ reported in the section above and Eq. (1). To do so the value of the inductance variation per unit length calculated according to Burton [20] and Kohlberg [21] will be used.

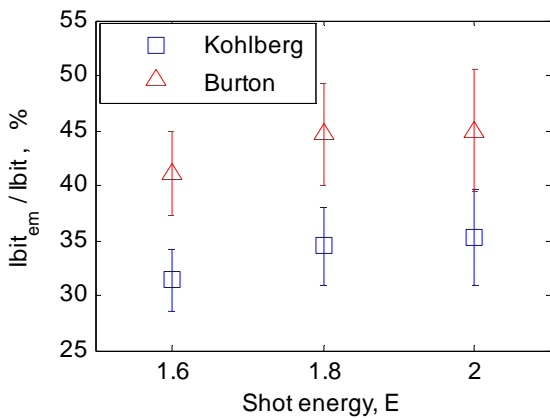


Figure 14: Electromagnetic to total Ibit ratio

Figure 14 shows the ratio between electromagnetic impulse bit values calculated with the values proposed for L' and the total measured impulse bit at the different tested energies. The data show that the electromagnetic contribution accounts for about 30 to 45 % of the total impulse bit in agreement with that measured in other thrusters [1, 14, 15, 22, 34].

Mass Bit and Specific Impulse Measurements

The thruster mass bit has been measured using a Mettler Toledo high precision scale with an accuracy of

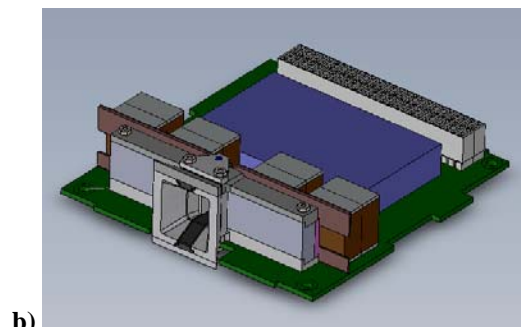
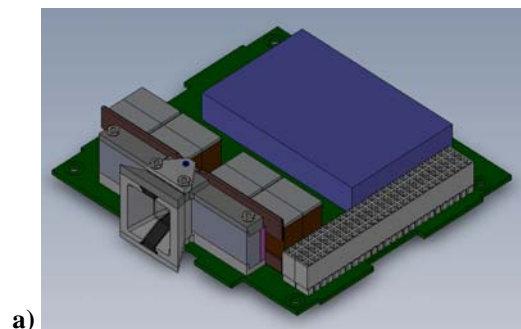
0.01 mg . The mass bit has been derived by the weighing the propellant bars before and after a sequence of hundreds of shots have been completed. Up to now measurements have been performed only at an energy of 1.8 J providing a repeatable value of the mass bit equal to $4.8 \pm 0.25 \mu\text{g}$. Using this value the specific impulse relative to the shot energy of 1.8 J can be estimated to be 590 ± 60 seconds and hence well above the I_{sp} required by the mission (410s). This specific impulse and impulse bit translate into an efficiency of about 5%. The reason of this poor efficiency can be found in the high initial inductance of the capacitor bank and in the presence of sidewalls that have been found to negatively affect the performances of a PPT [23]; the electrodes shape might also be a factor with tongue shaped electrodes being able to improve the electromagnetic contribution to the impulse bit.

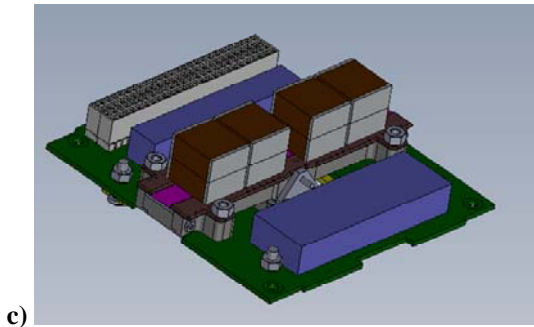
UKUBE1 RELATED ACTIVITIES

The PPT was selected as a candidate payload on board of the UKube1 mission and, in the light of this possibility, a series of simulations and tests have been performed.

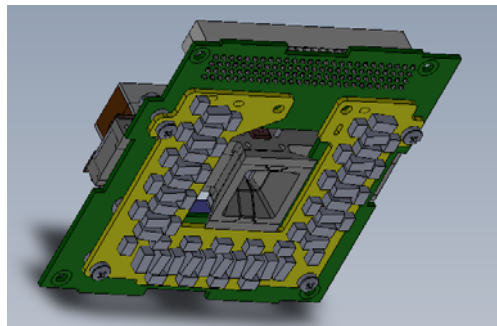
Thruster Module Configuration Redesign and Simulation

In the light of the UKube1 mission the PPT design has been reviewed and adapted to the UKube1 requirements [35]. Three different possible configurations have been produced depending on the direction along which the thruster will fire named X, Y and Z configuration (Figure 15).





c)

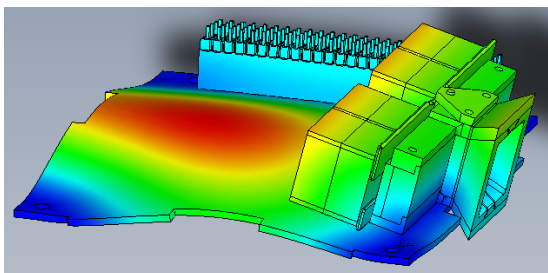


d)

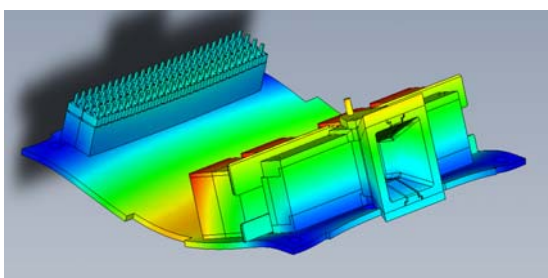
Figure 15: UKube1 PPT configurations. a) X configuration, b) Y configuration, c) Z top view, d) Z bottom view

The three solutions differ only for the PPT discharge chamber arrangement and for the propellant bars and supporting structure length. The key design parameters have been left untouched with respect to the ESA ITI PPT to avoid any change in thruster performance and/or reliability.

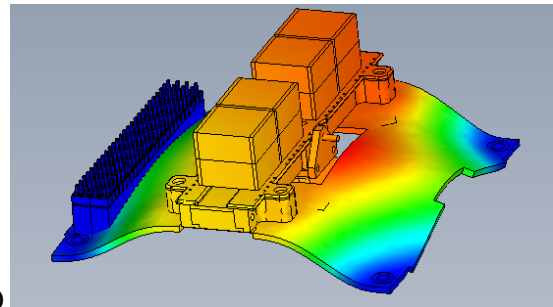
These three solutions have been simulated numerically to verify their lowest resonant frequency.



a)



b)



c)

Figure 16: PPT first resonant mode. A) X configuration $f = 212$ Hz, b) Y configuration $f = 185$ Hz, c) Z configuration $f = 240$ Hz

All the calculated natural frequencies have been found to be in excess of the UKube1 requirement of 150 Hz.

Thruster Chamber Vibration Test

From the numerical simulations the Y configuration resulted to be the less stiff hence it has been selected of vibration testing. The goal of the testing is twofold: first to measure the vibration frequencies of the thruster and compare them to the numerical predictions and second to verify the structural resistance of the discharge chamber. The concern regarding the discharge chamber is posed by the brittleness of the material (Macor®) used to manufacture most of the parts it is made of.

To perform such a test, one of the existing discharge chambers has been mounted on a PC104 board with dummy masses used to simulate the electronics. In Table 2 a comparison between the parts used for the test and the one to be used on the UKube 1 payload is reported to verify the validity of the tests.

Table 2: Vibrational test payload components

UKube 1 “flight” component	Vibration test component	Comments
Discharge chamber	ITI spare discharge chamber	Fully representative
Busbars	ITI spare busbars	Fully representative
Capacitor bank	ITI spare “test” bank	Representative in terms of volume. Weaker connection to the busbars (leaded capacitors). Higher mass.
PC104 board	Commercial PCB	representative
Electronics	Dummy mass (bolts)	Representative in terms of mass and mass distribution

As it can be seen from Table 2 the model to be tested is representative of the proposed UKube payload. The only strong difference lies in the capacitor bank. In

particular the capacitors to be used on board UKube 1 will be surface mount capacitors whereas the for the vibrational test the “test capacitor bank” made of tin leaded capacitor will be used. This means that during these tests low natural frequencies associated with the capacitors movement are to be expected whereas such frequencies will not be present once the selected capacitors will be used. Considering the tin leads as cantilever beams their first two resonant frequencies can be numerically estimated to be 86 and 92 Hz.

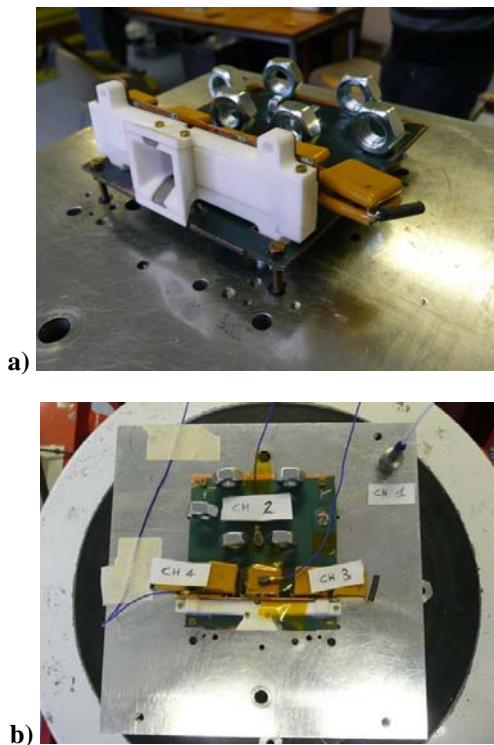


Figure 17: a) Vibrational tests setup. b) accelerometers positions

The first tests consisted in a sine sweep of the payload along the X, Y and Z directions to verify its natural frequencies. The results are quickly reported in Figure 18 where the position of the sensors is reported in Figure 17 b.

The first two peaks found in Figure 18 are relative to resonance in the capacitor bank and the frequencies values are in good agreement with the ones calculated numerically, as already said these structural modes will not be present once the “flight” capacitors will be used. The first resonant frequency of the structure is at about 186 Hz. This result is confirmed by numerical simulations carried out on the 3D model of the payload that computed a first natural frequency of 185 Hz and a second natural frequency of 361 Hz.

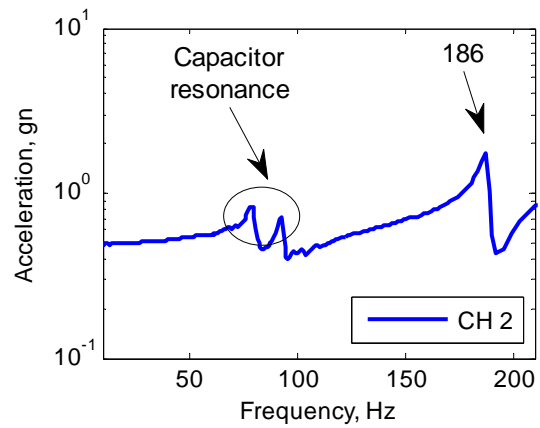


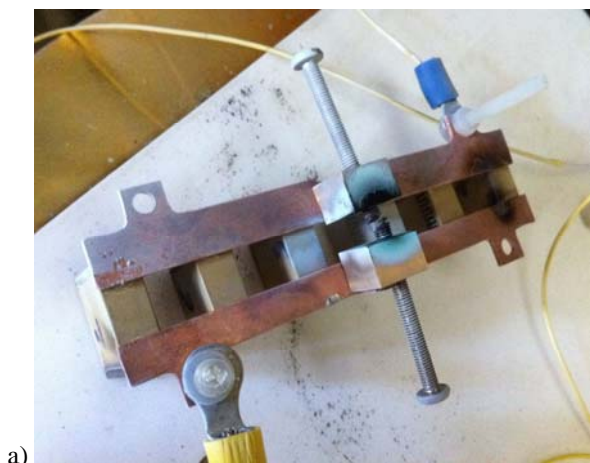
Figure 18: Frequency sweep output

Capacitor Change and Lifetime Test

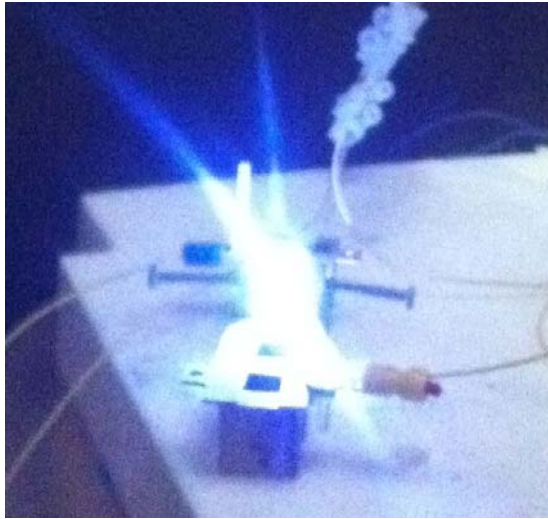
Given the premature failure of the “flight” capacitor bank a market survey to find suitable capacitors have been performed. Suitable ceramic surface mount capacitors with an energy density of 0.38J/cm² have been found and life tested using the University of Southampton facilities.

The capacitors have been mounted on the thruster bus bars connected to two screws acting as electrodes so that the electrode gap can be varied to obtain a discharge at the desired voltage (Figure 19) . The capacitors have been fired with a frequency of about 1 – 2 Hz and a charge voltage in the range 80 – 100% of their rated voltage recording peak currents in excess of 5kA.

Up to date the capacitors have successfully completed 1,500,000 shots and they are still fully operational. The test is still ongoing and will be continued until the capacitors failure.



a)



b) **Figure 19: Capacitors lifetest. a) setup, b) firing**

CONCLUSIONS AND FUTURE WORKS

The design of a Pulsed Plasma Thruster for Cubesat applications has been presented. The ultimate goal of this project is to design a PPT able to double the lifetime of a Cubesat on a 600-km orbit.

The thruster configuration, electrode dimensions and propellant mass have been selected in order to comply with the tight constraints on the dimensions and mass budget present on a Cubesat. Particular attention has been paid to the E/A ratio since the choice of this value has been found to influence the Isp produced by the thruster and hence is key in meeting the mission requirements. The design of the spark plug needed to initiate the PPT discharge was also presented.

The thruster has been tested to verify its performances measuring its current and voltage waveforms, impulse bit and mass bit. The thruster has shown damped oscillatory discharge behaviour with peak current in the range of 5-10kA depending on the shot energy. The thruster has also been able to provide impulse bits up to 34 μNs with a specific Ibit of about 17 $\mu\text{Ns/J}$. The mass bit has been measure at a shot energy of 1.8 J and a specific impulse of about 600 s has been obtained. Such value is well in excess of the requirement of 410 s.

The completely operational assembled thruster including electronics, structural support and the capacitor bank (using the flight capacitor bank) presented a total mass of about 160g hence very close to the target of 150g. It can be concluded that up to this point the design has proven to be satisfactory with the thruster able to meet the tight mass and volume budget and able to provide performances in excess of the mission requirements.

The thruster has also been numerically simulated to verify its natural frequencies and its compliance with the UKube 1 requirements. Actual vibrational test have been carried out confirming the numerical simulation and proving the discharge chamber resistance to the launch loads.

New capacitors have also been found and life tested in representative conditions showing a lifetime in excess of 1,500,000 shots.

Future works will consist in completing the mass bit measurements to get a more complete picture of the Isp trend with shot energy. A second flight bank is also to be assembled soon and the current, voltage and mass bit measurements will be repeated using this bank. The use of a lower inductance capacitor bank should improve the performances of the PPT producing a higher peak current and hence pushing the plasma away from the ablating surface more rapidly hence reducing the ablated mass, improving the ionization fraction and ultimately increasing Isp and efficiency [12, 22]. In particular assuming an initial inductance of about 3 nH (in agreement with the value extrapolated from Figure 8) peak currents of about 15-20kA will be obtained and according to Eq. (6) a significant increase in Ψ is to be expected with a consequent sensible increase in efficiency.

Acknowledgments

The authors would like to thank Mr. Matthias Lau and Prof. G. Herdrich for the great help provided in performing the impulse bit measurements at Institute of Space Systems, University of Stuttgart, Germany.

References

1. R.L.Burton and P.J.Turchi, "Pulsed Plasma Thruster", Journal of Propulsion and Power, Vol. 14, No. 5, 1998
2. W.J.Guman and D.M.Nathanson, "Pulsed Plasma Microthruster Propulsion System for Synchronous Orbit Satellite", Journal of Spacecraft, 7, 4, 1970
3. W.J.Guman and T.E.Williams, "Pulsed Plasma Microthruster for Synchronous Meteorological Satellite (SMS)", The 10th International Electric Propulsion Conference, Lake Tahoe, Nevada, USA, October 31-November 2, 1973
4. C.Rayburn, M.Campbell, W.A.Hoskins, and R.J.Cassady, "Development of a Micro Pulsed Plasma Thruster for the Dawgstar Nanosatellite", AIAA Paper 2000-3256, 2000

5. R.J.Cassady, W.A.Hoskins, M.Campbell, and C.Rayburn, "A Micro Pulsed Plasma Thruster (PPT) for the "Dawgstar" Spacecraft", IEEE 0-7803-5846-5, 2000
6. M.Igarashi, N.Kumagai, K.Sato, K.Tamura, H.Takegahara, H.Okamoto, T.Wakizono, and H.Hashimoto, "Performance Improvement of Pulsed Plasma Thruster for Micro Satellite", The 27th International Electric Propulsion Conference, Pasadena, CA, 15-19 October, 2001
7. H.Takegahara, M.Igarashi, N.Kumagai, K.Sato, K.Tamura, M.Sugiki, and H.Hashimoto, "Evaluation of Pulsed Plasma Thruster System for μ -Lab Sat II", The 27th International Electric Propulsion Conference, Pasadena, CA, 15-19 October, 2001
8. N.Kumagai, K.Sato, K.Tamura, K.Kawahara, T.Koide, H.Takegahara, M.Sugiki, T.Wakizono, and H.Hashimoto, "Research and Development Status of Low Power Pulsed Plasma Thruster System for μ -Lab Sat II ", The 28th International Electric Propulsion Conference, Toulouse, France, 17-21 March, 2003
9. J.Iio, J.Uezu, T.Fukushima, Y.Kamishima, and H.Takegahara, "Evaluation on Impulse Bit Characteristics of Pulsed Plasma Thruster by Single Impulse Measurement", The 29th International Electric Propulsion Conference, Princeton University, October 31- November 4, 2005
10. Cal Poly, "CubeSat Design Specification Rev. 12", 2010
11. J.Ziemer, E.Y.Choueiri, and D.Birx, "Comparing the Performance of Co-Axial and Parallel-Plate Gas-Fed PPTs.", IEPC-99-209, 26th International Electric Propulsion Conference, 1999
12. A.Nawaz, R.Albertoni, and M.Auweter-Kurtz, "Thrust efficiency optimization of the pulsed plasma thruster SIMP-LEX ", Acta Astronautica, 67, 2010
13. P.Shaw and V.Lappas, "Modeling of a Pulsed Plasma Thruster; Simple Design, Complex Matter", Space Propulsion 2010, San Sebastian, Spain, 2010
14. W.J.Guman and T.E.Williams, "Pulsed Plasma Microthruster for Synchronous Meteorological Satellite (SMS)", The 10th International Electric Propulsion Conference, Lake Tahoe, Nevada, USA, October 31- November 2, 1973
15. R.J.Vondra, K.Thomassen, and A.Solbes, "Analysis of Solid Teflon Pulsed Plasma Thruster", Journal of Spacecraft and Rockets, Vol. 7, No. 12, 1970
16. W.J.Guman, R.J.Vondra, and K.Thomassen, "Pulsed Plasma Propulsion System Studies", AIAA Paper 70-1148, 1970
17. R.J.Vondra, K.Thomassen, and A.Solbes, "A Pulsed Electric Thruster for Satellite Control", Proceedings of the IEEE, Vol 59, No 2, 1971
18. R.J.Vondra and K.Thomassen, "Performance Improvements in Solid Fuel Microthrusters", Journal of Spacecraft and Rockets, Vol. 9, No. 10, 1972
19. R.J.Vondra and K.Thomassen, "Flight Qualified Pulsed Electric Thruster for Satellite Control", Journal of Spacecraft and Rockets, Vol. 11, No. 9, 1974
20. R.L.Burton, M.J.Wilson, and S.Bushman, "Energy Balance and Efficiency of the Pulsed Plasma Thruster", AIAA-1998-3808, AIAA/ASME/SAE/ASEE Joint Propulsion Conference and Exhibit, 34th, Cleveland, OH, July 13-15, 1998
21. I.Kohlberg and W.O.Coburn, "A Solution for Three Dimensional Rail Gun Current Distribution and Electromagnetic Fields of a Rail Launcher", IEEE Transactions on Magnetics, 31, 1995
22. R.Jahn, "Physics of Electric Propulsion", McGraw-Hill, New York, 1968
23. J.Ziemer, "Performance Scaling of Gas-Fed Pulsed Plasma Thrusters", Ph.D.Thesis, Department of Mechanical and Aerospace Engineering, Princeton University, 2001
24. D.J.Palumbo and W.J.Guman, "Continuing Development of the Short Pulsed Ablative Space Propulsion System", AIAA-72-1154, AIAA-SAE 8th Joint Propulsion Conference, New Orleans, 1972
25. W.J.Guman, "Designing Solid Propellant Pulsed Plasma Thruster", AIAA-1975-410, 11th Electric Propulsion Conference, 1975
26. P.Gessini and G.Paccani, "Ablative Pulsed Plasma Thruster System Optimization for Microsatellites", 27th International Electric Propulsion Conference, IEPC-01-182, 2001
27. P.Gessini, R.Intini Marques, S.B.Gabriel, and S.M.Veres, "Propulsion System Optimization for

Satellite Formation Flying", 4th International Workshop on Satellite Constellations and Formation Flying, INPE, São José dos Campos, Brazil, 2002

28. M.E.Brady and G.Aston, "*Pulsed Plasma Thruster Ignitor Plug Ignition Characteristics*", Journal of Spacecraft and Rockets, Vol. 20, No. 5, 1983

29. R.Intini Marques and S.B.Gabriel, "*High Frequency Burst Pulsed Plasma Thruster Research at the University of Southampton*", IEPC-2007-300, 30th International Electric Propulsion Conference, Florence, Italy September 17-20, 2007

30. D.J.Palumbo and W.J.Guman, "*Propellant Sidefeed-Short Pulse Discharge Thruster Studies*", Fairchild Industries, Inc., N72-20756, Farmingdale, NY, 1972

31. A.Nawaz, M.Auweter-Kurtz, G.Herdrich, and H.Kurtz, "*Investigation and Optimization of an Instationary MPD Thruster at IRS*", 29th International Electric Propulsion Conference, Princeton University, 2005

32. A.Nawaz, G.Herdrich, H.Kurtz, T.Schönherr, and M.Auweter-Kurtz, "*SIMP-LEX: Systematic Geometry Variation Using Thrust Balance Measurements*", 30th International Electric Propulsion Conference, Florence, Italy September 17-20, 2007

33. A.Nawaz, M.Auweter-Kurtz, G.Herdrich, and H.Kurtz, "*Experimental Setup of a Pulsed Plasma Thruster at IRS*", European Conference for Aerospace Sciences (EUCASS), 2005

34. G.Paccani, L.Petrucci, and W.D.Deininger, "*Scale Effects on Solid-Propellant Coaxial Magnetoplasmadynamic Thruster Performance*", Vol 19, No 3, 2003

35. UKube Payload Interface Document, Issue 3, 2011

36. PPTCUP Payload Interface Document, 2011

37. <http://www.ukspaceagency.bis.gov.uk/19128.aspx>, 2011